Self-Similar Interfacial Impedance of Electrodes in High Conductivity Media

Anil Koklu[1,*], Amin Mansoorifar[1], Jason Giuliani[2], Carlos Monton[2], Ali Beskok[1]

[1]*Department of Mechanical Engineering, Southern Methodist University, Dallas, TX 75205, USA*

[2]*Department of Physics and Astronomy, University of Texas at San Antonio, TX 78249, USA*

akoklu@smu.edu

Objectives

- Electrodes have been widely used for dielectric spectroscopy, electrochemical sensing, bio-potential recording, and neural stimulation applications.
- Well-characterized time scales elucidating the electrode polarization (EP) effect are important for the rational design of microfluidic devices and impedance sensors.
- In this study, we systematically investigate the characteristic time scales of diffuse charge dynamics for disc shape planar and porous electrodes considering channel height, electrode diameter, and Debye length effects on characteristic time scale in a binary electrolyte solution.

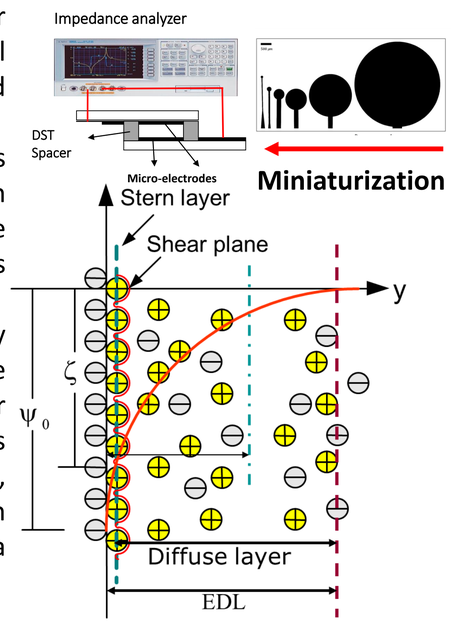

Theory

Parallel Plate Disc Electrodes

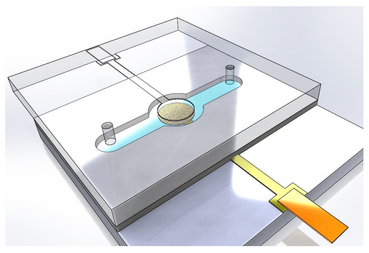

The primary time scale : $\tau_c = \lambda H/D$

λ: Debye Length (m)

h: Channel Height (m)

D: Diffusion Coefficient (m^2/s)

Solution Resistance: $R_{sol} = H/(\sigma_b A)$

σ_b: Bulk Conductivity (S/m)

A: Geometric Surface Area (S/m)

Single Disc Electrode

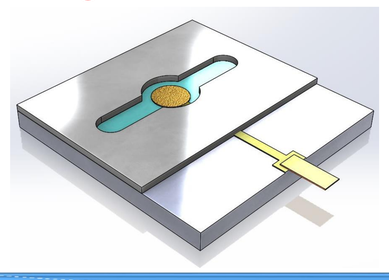

The primary time scale : $\tau_c = \lambda \phi/D$

ϕ: Electrode Diameter (m)

Solution Resistance: $R_{sol} = 1/(2\sigma_b \phi)$

$$\lambda = \sqrt{\frac{\varepsilon RT}{\sum_{i=1}^{N} z_i^2 F^2 c_i}}$$

$f^* = f \times \tau_c$ f: Frequency (Hz)

f^*: Dimensionless Frequency

Numerical Simulations

Nernst-Planck Equation:

$$\frac{\partial c_i}{\partial t} + \nabla \cdot \left(-D_i \nabla c_i - z_i D_i^2 F c_i \nabla \psi / RT\right) = 0$$

Poisson Equation:

$$\nabla \cdot \varepsilon \boldsymbol{E} = F \sum_i z_i c_i$$

Applied Potential:

$$\psi = \psi^{AC} \sin(\omega t)$$

Measured Current:

$$\boldsymbol{J} = F \int \sum_i z_i \boldsymbol{J}_i = \mathrm{J} \sin(\omega t - \varphi)$$

Measured Impedance:

$$Z = \frac{\psi}{J} = \left|\frac{\psi^{AC}}{\mathrm{J}}\right| \angle\varphi = |Z| \angle\varphi$$

Simulation Domain

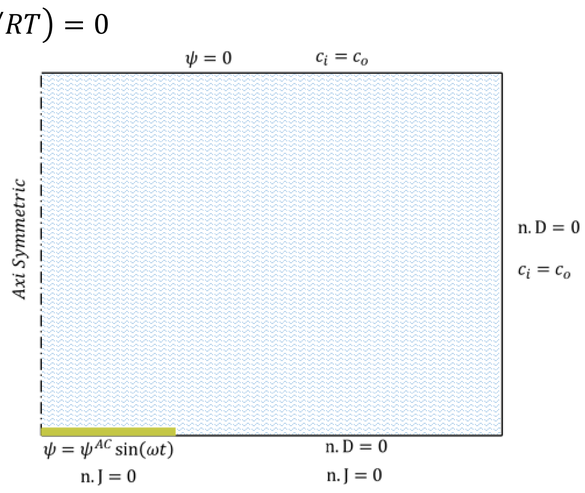

Device Fabrication

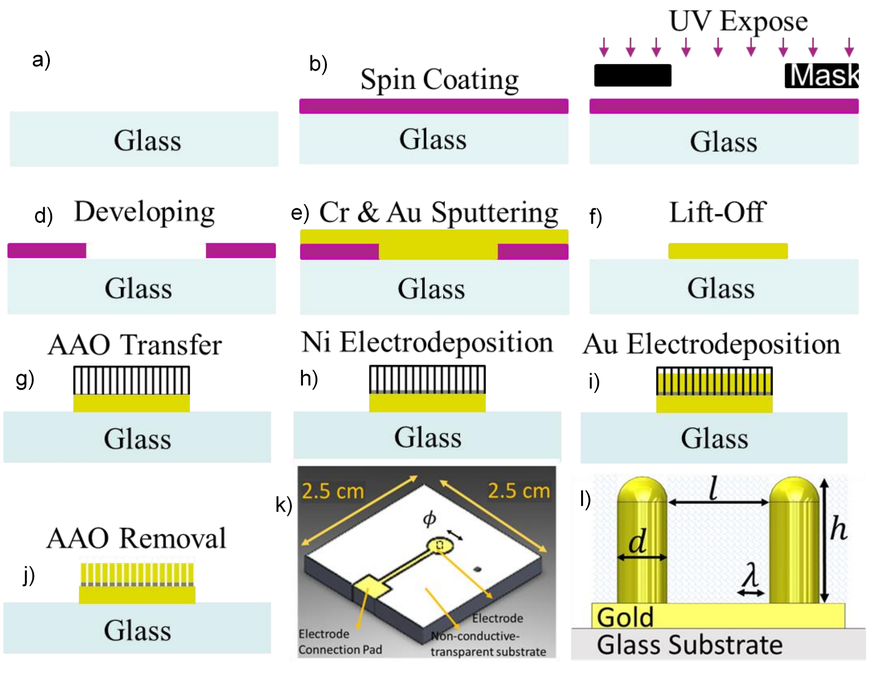

- Process flow of electrode fabrication (a-j) and schematics of gold disc electrode with relevant dimensions (k). The GP electrode surface is coated with cylindrical GNr with known height (h), diameter (d) and separation distance (l), and λ is the Debye length (l).

Results for Parallel Plate Electrodes Configuration

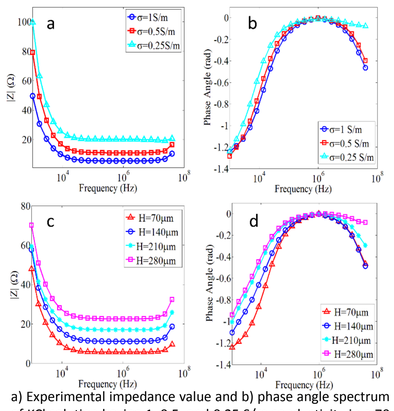

a) Experimental impedance value and b) phase angle spectrum of KCl solution having 1, 0.5, and 0.25 S/m conductivity in a 70 µm channel height. c) Experimental impedance value and d) phase angle spectrum of 1 S/m KCl solution in micro-channels having 70, 140, 210, and 280 µm height.

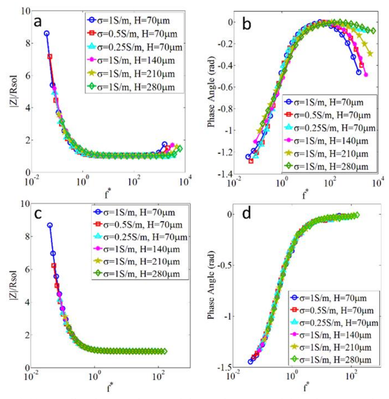

a) Normalized experimental impedance and b) phase angle spectrum as a function of the normalized frequency. c) Normalized numerical impedance and d) phase angle spectrum as a function of the normalized frequency

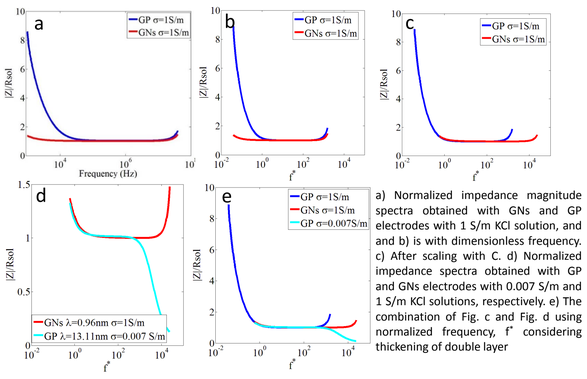

a) Normalized impedance magnitude spectra obtained with GNs and GP electrodes with 1 S/m KCl solution, and and b) is with dimensionless frequency. c) After scaling with C. d) Normalized impedance spectra obtained with GP and GNs electrodes with 0.007 S/m and 1 S/m KCl solutions, respectively. e) The combination of Fig. c and Fig. d using normalized frequency, f* considering thickening of double layer

$$\tau_n = C\tau_c$$

$$\lambda_{eff} = C\lambda$$

C is a dimensionless coefficient which might be a function of porosity, thickness of nanostructures, tortuosity, or combination of these parameters.

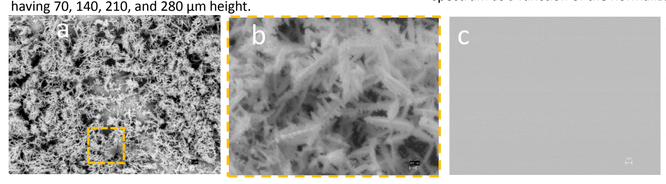

SEM images of GNs (a, b) structured and GP (c) electrodes at different magnification factors. Scale bars in Figure (a), (b), and (c) are 2 µm, 300 nm, and 1 µm, respectively.

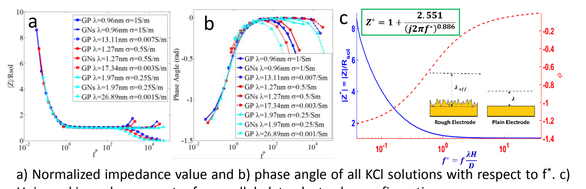

a) Normalized impedance value and b) phase angle of all KCl solutions with respect to f*. c) Universal impedance spectra for parallel plate electrodes configuration.

Results for Single Electrode Configuration

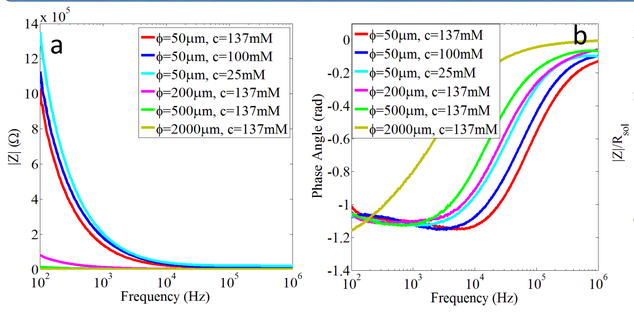

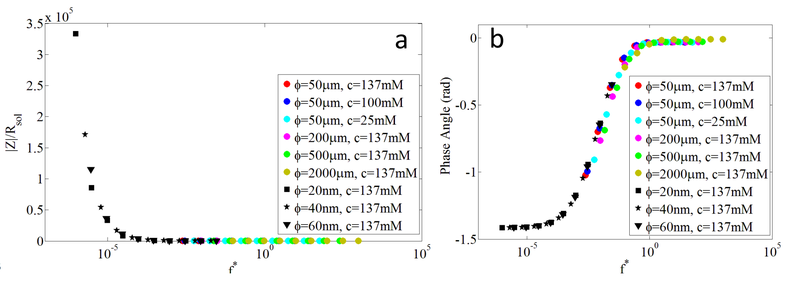

(a) Normalized numerical impedance and (b) phase angle spectrum as a function of the dimensionless characteristic frequency.

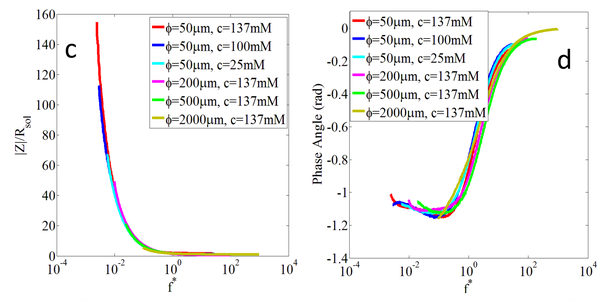

(a) Experimental impedance value and (b) phase angle spectrum at various KCl concentrations and for different electrode diameters. (c) Normalized experimental impedance and (d) phase angle spectrum as a function of the dimensionless frequency.

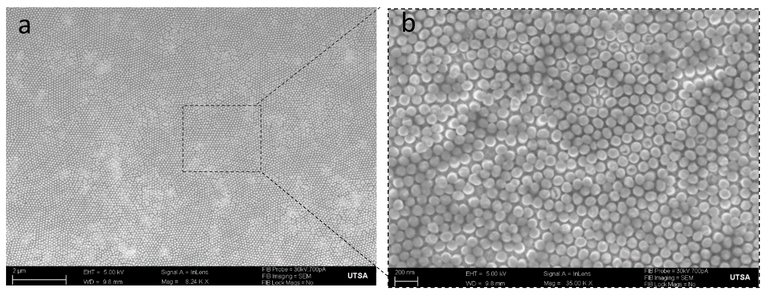

Figure 4. SEM images of GNr structured electrodes at different magnification factors. Scale bars in Figure (a) and (b) are 2 µm and 0.2 µm, respectively.

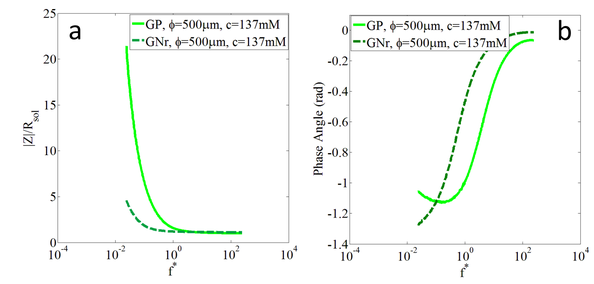

Normalized impedance values (a) and phase angles (b) obtained with GP (solid line) and GNr (dashed line) electrodes at 137mM KCl solution.

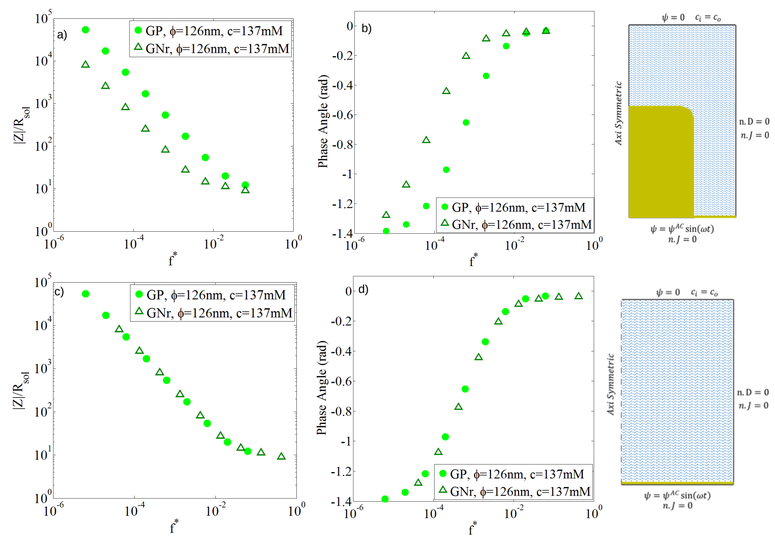

Figure 8. Normalized impedance values (a) and phase angles (b) obtained with GP (circles) and GNr (triangles) electrodes at 137mM KCl solution. Normalized impedance values (c) and phase angles (d) after the dimensionless frequency of GNr is multiplied with the surface enlargement factor (C = 6.6).

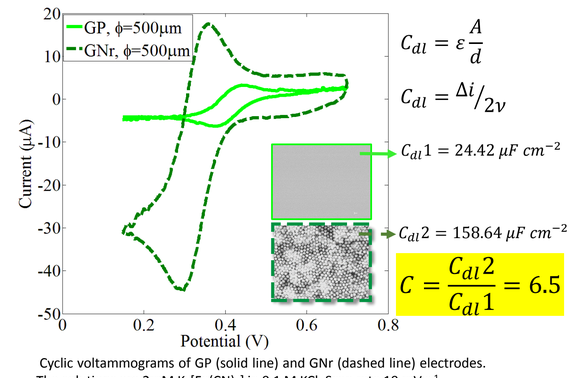

Cyclic voltammograms of GP (solid line) and GNr (dashed line) electrodes. The solutions are 2mM $K_3[Fe(CN)_6]$ in 0.1 M KCl. Scan rate 10 mV s^{-1}.

$$\tau_n = C\tau_c$$

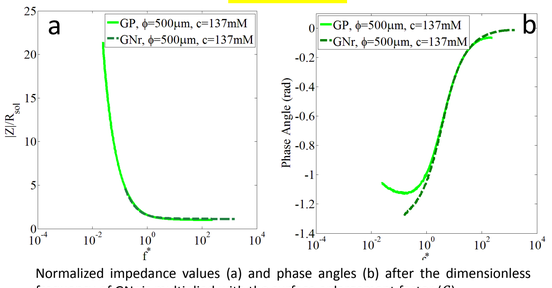

Normalized impedance values (a) and phase angles (b) after the dimensionless frequency of GNr is multiplied with the surface enlargement factor (C).

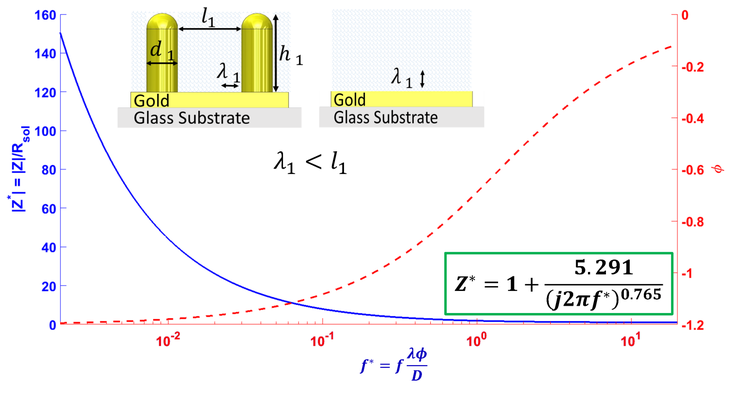

Universal impedance spectra for single electrode configuration.

Conclusion

- Impedance spectra for different electrode diameters, channel heights and solution conductivities were experimentally and numerically investigated and self-similar impedance spectra was obtained by using τ_c as a primary time scale of EP behavior for planar electrodes.
- Template based electrochemical deposition technique was used to generate gold nanorods on planar electrodes to examine the effect of area increase on EP. The results revealed that normalized impedance spectra of GNr electrodes collapsed to the impedance spectra obtained with gold planar electrodes after scaling with surface enlargement factor ($\tau_n = C\tau_c$) .
- The defined characteristic time scales enables to identify the limitations of electrode/electrolyte system and predict the system EP behavior for both planar and rough electrodes prior to fabrication and experimentation.
- In the future studies, GNr structured electrodes with different nanorod separation distances but same effective surface area will be used to determine the EDL overlap effect on EP.

Publications:

(1) A. Koklu, A. Mansoorifar, A. Beskok, Self-Similar Interfacial Impedance of Electrodes in High Conductivity Media. ACS Analytical Chemistry, DOI:10.1021/ acs.analchem. 7b03753, 2017.

(2) A. Koklu, A. Mansoorifar, Jason Giuliani, Carlos Monton, A. Beskok, Self-Similar Interfacial Impedance of Electrodes in High Conductivity Media II: Disc Electrodes. ACS Analytical Chemistry, 2018 (Under Review).